Received: 19 April 2024 | Accepted: 24 September 2024

DOI: 10.1002/vzj2.20387

Vadose Zone Journal

ORIGINAL ARTICLE

Simulating controlled drainage and hydrological connections in a cultivated peatland field

Aleksi Salla[1] | **Heidi Salo**[1] | **Mika Tähtikarhu**[2] | **Hannu Marttila**[3] | **Miika Läpikivi**[3] | **Maarit Liimatainen**[4] | **Timo Lötjönen**[4] | **Harri Koivusalo**[1]

[1]Department of Civil and Environmental Engineering, Aalto University School of Engineering, Aalto, Finland

[2]Natural Resources Institute Finland, Helsinki, Finland

[3]Water, Energy and Environmental Engineering Research Unit, University of Oulu, Oulu, Finland

[4]Natural Resources Institute Finland, Oulu, Finland

Correspondence
Aleksi Salla, Department of Civil and Environmental Engineering, Aalto University School of Engineering, P.O. Box 15200, FI-00076, Aalto, Finland.
Email: aleksi.salla@aalto.fi

Assigned to Associate Editor Andrea Carminati.

Funding information
Maa- ja Vesitekniikan Tuki Ry, Grant/Award Number: 700801

Abstract

Cultivated peatlands are increasingly regarded as hot spots due to climate change and other environmental concerns. Flexible water management, such as controlled drainage, is proposed to optimize cultivation and reduce environmental risks in peatland fields. The hydrological and environmental implications of controlled drainage depend on site-specific variables, and it is unclear how controlled drainage should be implemented in various conditions. Simulation models are a promising approach to systemically study the field hydrology, as models can capture the complete water balance, which is difficult through experimental studies alone. We calibrated and validated the spatially distributed model FLUSH to describe the hydrology of a field block with a shallow peat cover and controlled drainage in central western Finland. The objectives were to analyze the hydrological effects of controlled drainage and detect hydrological connections between the field and an adjacent upslope forest area. The results showed how inflow from the forest can induce high observed drain discharge but impacted the block groundwater tables only in the proximity of the forest (distance <25 m). The effect of controlled drainage on groundwater tables was on average 0.15 m and seasonally varying. Controlled drainage reduced drain discharge, and the reduction was larger with the forest area included in the model. While controlled drainage effects on groundwater levels and soil moisture were insensitive to groundwater influxes from adjacent areas, the water balance impact highlights the role of hydrological connections in the hydrology of cultivated peatlands under controlled drainage.

Plain Language Summary

Sustainable agriculture on peatlands requires water management that allows sufficient removal of excess water when needed by the cultivation practices while minimizing the negative environmental impacts of draining peatlands, especially

Abbreviations: CD, controlled drainage; GPR, ground-penetrating radar; KGE, Kling–Gupta efficiency; MAE, mean absolute error; OW, observation wells; SWE, snow water equivalent; WRC, water retention curve.

carbon dioxide emissions and nutrient leaching. One promising method for this is controlled drainage, a subsurface drainage method that enables controlling the amount of drainage, but more research is needed to better understand how cultivated peatlands respond to it. In this study, a computational model FLUSH was used to describe the flow and storage of water and how controlled drainage affects them on a cultivated peatland field in central western Finland. The model supported our hypothesis that the large observed drain discharge was caused by groundwater flow from an adjacent forest area. According to the model, the controlled drainage scheme that was applied in the field raised groundwater tables on average 0.15 m and reduced drain discharge.

1 | INTRODUCTION

Peatlands constitute a significant carbon stock, especially in boreal and subarctic regions, where peat contains 15%–30% of the global soil organic carbon (Limpens et al., 2008). Due to their large storage of water, efficient connections to surface water resources, and organic matter decomposition, peatlands play an important role in water and biochemical cycles (Rezanezhad et al., 2016). Agriculture is one of the most typical land use practices in peatlands (Oleszczuk et al., 2008), and especially in northern areas, where suitable mineral soil areas are limited, low-lying peatlands are exploited as arable land areas because of their high water holding capacity. In Nordic countries, 1,000,000 ha of peatlands are used for agriculture (Maljanen et al., 2010).

Farming in peatlands requires intensive soil drainage operations with consequences on local water balance and biochemical cycling (Pham et al., 2023; Regina et al., 2016; Yli-Halla, Lötjönen, Kekkonen et al., 2022). The drainage, conducted with subsurface drain installations or open ditches, is intended to lower groundwater table and at the same time it affects the water balance of the fields. Lowered groundwater tables in peatlands have been associated with peat degradation leading to soil subsidence, increased carbon dioxide (CO_2) emissions, and nutrient leaching (Evans et al., 2021; Holden et al., 2004; Ikkala et al., 2021; Laiho, 2006; Maljanen et al., 2010; Yli-Halla, Lötjönen, Kekkonen et al., 2022), and drain discharge is a major pathway for the export of nutrients to surface waters (Coelho et al., 2020). The consequent challenge of drainage design is to simultaneously consider both agricultural productivity and environmental aspects of drainage procedures.

Controlled drainage (CD) allows temporal adjustment of the drainage outlet elevation (and consequently drainage depth) to cope with different hydrological conditions and drainage requirements, which makes it an attractive method to reduce the environmental impacts of cultivated peatlands. However, the feasibility of CD depends on local meteorological and hydrological variables and site conditions, including topography and soil properties (Joel et al., 2009; Salo et al., 2021). While hydrological impacts of CD have been studied in mineral soils in different locations (e.g., Dou et al., 2022; Kęsicka et al., 2023; Salo et al., 2021; Youssef et al., 2021), there is a knowledge gap in how cultivated peatlands respond to CD schemes, and what the main factors affecting water balance are in peatland fields under CD. Hydrological observations in peatland areas are challenged by existence of complex interactions within the peatland. Implications of field drainage are often studied with field-scale measurement campaigns (e.g., Turunen et al., 2013; Yli-Halla, Lötjönen, Kekkonen et al., 2022) and the data alone provide limited mechanistic view on the interactions. Therefore, hydrological knowledge based on combination of experimental and computational approaches is essential to gain sufficient knowledge for local and regional-scale water management in cultivated peatlands.

Peat is characterized by a strong dual porous nature (Rezanezhad et al., 2016), and macropores in peat have been shown to be important in runoff generation (Holden, 2009). The water balance of a drained peatland field is on the first hand controlled by meteorological conditions, the drainage system, thickness and hydraulic properties of the peat layer, hydraulic properties of the underlying mineral soil, vegetation, and topography. In addition, lateral groundwater flow through field boundaries can be an important factor in the field water balance, but it is often viewed only as an outflow component in the literature (e.g., Li et al., 2017; Muma et al., 2017; Turunen et al., 2013; Youssef et al., 2021). Together with deeper groundwater tables caused by drainage, lowered soil surface elevation due to prolonged drainage practices and peat degradation can make agricultural peatland fields more susceptible to groundwater inflow from adjacent areas. Especially groundwater flow through more permeable and macroporous upper layers of peat can have a strong impact on local water balance (Lambert et al., 2022; Päivänen, 1973). The presence of lateral groundwater inflow can

have practical implications in drainage design, as, for example, Koivusalo et al. (2008) found that ditch cleaning in a peat forestry catchment increased water flow into the catchment from the adjacent untreated control area. The impacts of such hydrological connectivity on the field water balance and the effects of CD have been rarely quantified, and the impacts are challenging to disentangle with field observations alone. Understanding of hydrological factors underpinning the efficiency of CD in different conditions can also provide information for targeting the measures within landscapes.

Combined with field observations, hydrological simulation models are an attractive approach to study the complete water balance, gain deeper insight on the hydrological processes, and test hypothetical water management schemes. Earlier modeling studies in managed peatlands have mainly focused on regional or catchment scales (e.g., Querner et al., 2010, 2012) and forestry sites (e.g., Haahti et al., 2016; Koivusalo et al., 2008). To our knowledge, field-scale multidimensional modeling studies of cultivated peatlands with sub-drainage system have not been done. Several field-scale simulation studies have been conducted in agricultural mineral soils applying conceptual and one-dimensional (1D) models (e.g., Knisel & Turtola, 2000; Larsson & Jarvis, 1999), two-dimensional (2D) models (e.g., Salo et al., 2021; Skaggs et al., 2004), and three-dimensional (3D) models (e.g., Turunen et al., 2013; Zhou et al., 2013). Unlike conceptual and 1D models, 3D models can account for spatial variability and are better suited for studying the hydrological interactions between areas.

The objective of this study was to (1) quantify the effects of CD on groundwater table depths, drain discharge, and peat moisture in a cultivated field block next to a forest area with higher soil surface elevation and (2) detect the existence and role of groundwater inflow from the forest on the field hydrology. A 3D dual-permeability hydrological model FLUSH was calibrated and validated against field observations under CD, and the results were compared to a simulated scenario of conventional subsurface drainage. The impact of hydrological connections between the field and the forest was assessed by comparing simulation results with and without the forest.

Core Ideas

- Combined with limited dataset, FLUSH provided a transparent tool to quantify the hydrology of a cultivated peatland.
- Hydrological connections had a strong impact on the field water balance but not on groundwater tables.
- Controlled drainage reduced groundwater table depths on average 0.15 m but had a small impact on peat moisture.
- Complex interactions within peatlands are a challenge for reproducing point observations with a model.

2 | MATERIALS

2.1 | Site description

The Ruukki research station, maintained by the Finnish Natural Resource Institute (Luke), is in the municipality of Siikajoki in central western Finland, 26 km from the coast of the Bothnian Bay (Figure 1). During the years 2014–2023, the average yearly temperature and precipitation in the region were 3.8°C and 574 mm annum^{-1}, respectively. Monthly averages are shown in Figure 2. The experimental field named NorPeat is 19.56 ha of arable land divided into six blocks with an average slope of ~0.2% (Pham et al., 2023). It is surrounded by similar arable land and bound by a forest area in the north-eastern end. The field is covered with a shallow (15–75 cm) layer of sedge peat mixed with coarse silt, below which there is acid sulfate mineral soil consisting of silty soil on top and clayey soil at the bottom. The area has been under agricultural use circa 100 years, and during that time it has been used for grass and cereal cultivation. The experimental field was established in 2016 for monitoring greenhouse gas emissions and leaching of substances (Yli-Halla, Lötjönen, Kekkonen et al., 2022). This study focuses on the hydrology of Block 1 (Figure 1), a 2.97 ha area with the thickest peat layer (45–75 cm) of the field blocks. The forest has higher soil surface elevation compared to the field (~1.2 m), and it is drained with ~0.7-m deep open ditches (spacing ~35 m) (National Land Survey of Finland, 2015). The forest is surrounded mostly by arable land and connects to wetland areas roughly 3 km from the field. The field and the forest share a 215-m-long border.

The field block is drained with controlled subsurface drainage. During the simulation period (2018–2021), there was a deeper open ditch at the north-western end of the block (Ditch 1 in Figure 1), and a shallower open ditch between the block and the forest (Ditch 2 in Figure 1). At the time of the establishment of the experimental field, the drainpipes in Block 1 and Block 2 (on the south-eastern side of Block 1) were renewed. In the renovation process, lateral drains (Ø 65 mm) were placed at a depth of 1.1–1.3 m with drain spacing of 12 m and with gravel as the envelope material (6.5 m^3 of gravel per 100 m of drainpipe). The drainage depth is clearly below the peat cover, with drainpipes mostly lying in the silty soil layer. Lateral drains are connected to a collector pipe (Ø 160 mm) leading to a control well (subsurface drainage outlet in Figure 1), where the drain outlet elevation can be controlled (Yli-Halla, Lötjönen, Kekkonen et al., 2022).

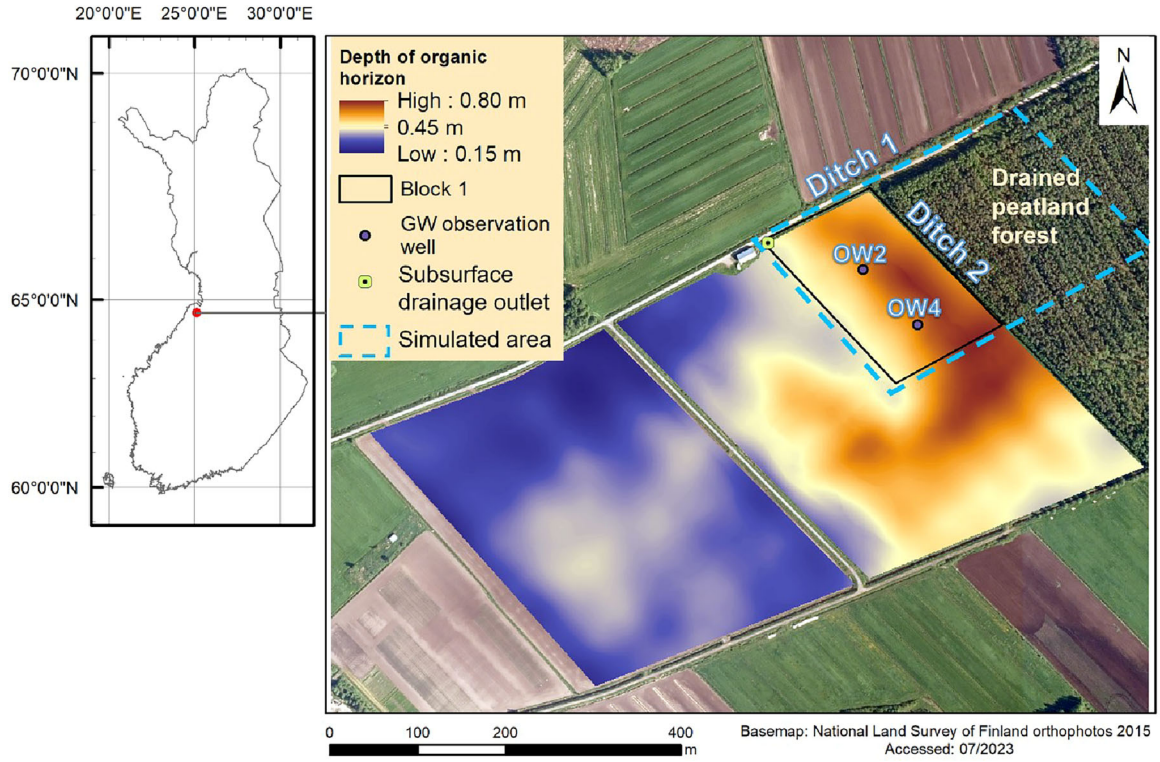

FIGURE 1 The location of the Ruukki research station, the depth of organic horizon in the cultivated area, and the locations of Block 1, the open ditches, the groundwater (GW) table observation wells (OWs), the subsurface drainage outlet, and the simulated area.

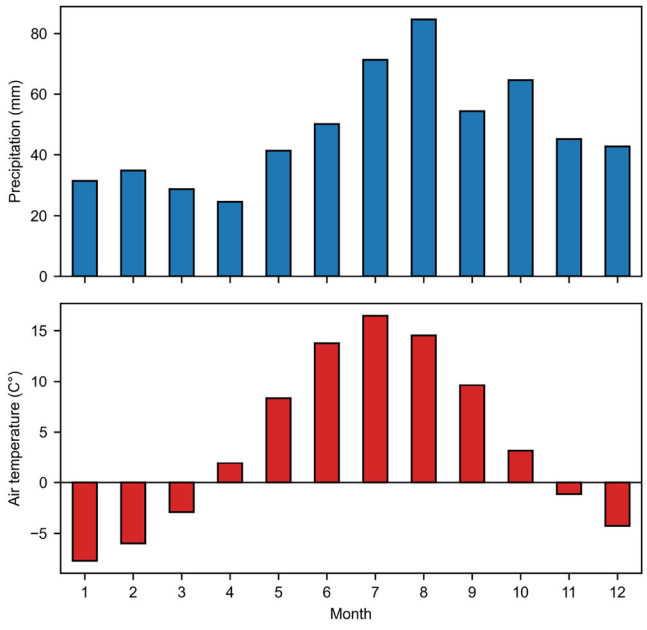

FIGURE 2 Average monthly precipitation and air temperature in Ruukki during 2014–2023.

2.2 | Data description

The key measurements included drain discharge, groundwater table depths, meteorological variables, soil hydraulic properties, soil moisture, and depth of the organic horizon. Drain discharge was measured automatically every 15 min using V notch weirs and pressure probes (STS PTM/N). At the measurement station well, water is pumped away from the well because the water level outside of the well is higher than drainage pipe outlets. In addition to a 2.5 kW electrical discharge pump, a tractor-driven hydraulic pump was used during flooding periods. Compared to a set of manual experiments conducted in 2017, there was an unsystematic error of 10%–30% in the automatic measurements, the absolute error having a negative correlation with the amount of drain discharge. (Yli-Halla, Lötjönen, Joki-Tokola et al., 2022).

Groundwater table depths were measured from two observation wells (OWs) in the block reaching the depth of 2 m (OW2 and OW4 in Figure 1). Both wells are located in the middle of two adjacent drainpipes at distances of 47 m (OW 2) and 172 m (OW 4) from the north-western end of the block. In addition to infrequent manual measurements, groundwater table depths were automatically measured every 15 min with Solinst Levelogger probes.

Hourly observations of air temperature, precipitation, wind speed, relative humidity, downward shortwave radiation, and snow depth were made at the site by the Finnish Meteorological Institute. In addition to seven snow water equivalent (SWE) measurements conducted during the study period, observed SWE was approximated from the observed snow depth. A crude approximation of SWE being half of snow depth was used, which is in line with Hill et al. (2019). The approximation was found to reflect individual field measurements of SWE and was thus assumed to yield a sufficient picture of SWE dynamics, especially during the hydrologically crucial major melting events in spring.

A ground-penetrating radar (GPR) was used to measure the thickness of the organic soil layer in the block, and soil hydraulic properties were determined from one location of the block at a depth range of 0–70 cm. The measurements described the properties of four different vertical soil layers: three peat layers and one mineral layer. Water retention curves (WRCs) were measured for all four layers using 10 pressure values logarithmically from 0.01 to 50 m. The shares of macropores were estimated based on the pore volume drained with 0.1 m pressure, according to Jarvis (2007). Dry bulk densities and porosities were measured from the same soil samples. Saturated hydraulic conductivities were measured only for the top and bottom peat layers. Soil moisture was measured from the peat layers at depths of 0.1 and 0.5 m with Soil Scout soil moisture sensors, but the measurements covered only 45% and 10% of the study period at the depths of 0.1 and 0.5 m, respectively.

3 | METHODS

3.1 | FLUSH

FLUSH is a dynamic and spatially distributed model for describing the hydrology of drained agricultural fields (Warsta, 2011; Warsta et al., 2013). It has been used to study, for example, the performance of subsurface drainage systems with different installation methods (Salo et al., 2019), the impacts of terrain slope on field water balance (Turunen et al., 2015), combined effects of CD and open ditch damming (Isomäki et al., 2024), and nutrient and sediment transport in drained agricultural fields (Salo et al., 2015; Turunen et al., 2017).

The 3D subsurface flow domain applies a dual-permeability model, which means the total porosity in each cell of the 3D computational grid (x, y, and z dimensions) is divided into soil matrix and macropore domains to depict slow and fast flow regimes, respectively. In both pore systems and in saturated and unsaturated zones, lateral (x and y) and vertical (z) water flow between the cells is described with the 3D Richards equation. The Richards equations for both pore systems (Warsta, 2011, eqs. 38 and 39) are numerically solved in the 3D global solution using the forward finite difference method for the temporal components and the finite volume method for the spatial components. Water retention properties and unsaturated hydraulic conductivities are calculated with the van Genuchten (1980) model. Water exchange between soil matrix and macropore domains is treated as a sink/source term in the continuity equations depending on the direction of the exchange. The rate of exchange depends on the pressure difference and hydraulic conductivity between the domains (Gerke & van Genuchten, 1993; Warsta, 2011). In both pore systems, groundwater table depth is defined as the first level of unsaturation starting from the bottom, and therefore the model gives separate groundwater table depths for both matrix and macropore systems. The 2D overland flow is solved using the diffuse wave approximation of the Saint Venant equations. Evapotranspiration is computed based on potential evapotranspiration, prescribed rooting depth timeseries, and simulated soil moisture. Description of snow accumulation and melt based on energy balance has been added to the model, according to Koivusalo et al. (2001).

In the model, precipitation is first stored in depression storage on the soil surface and thereafter the water can infiltrate into both pore systems. The infiltration is computed based on Darcy's law (Warsta et al., 2013). If precipitation or/and snowmelt exceed the infiltration capacity and the depression storage is full, overland flow is initiated. Water can be removed from the model via evapotranspiration and groundwater outflow through model boundaries, open ditches, and subsurface drainpipes. Groundwater outflow can be described with a constant head type boundary condition or with a specified slope of the water table at the boundary. Open ditches and subsurface drainpipes act as local sinks, where the subsurface outflux in a computation cell containing a drainpipe or ditch segment is calculated as follows:

$$q = AK_s \frac{H_c - \left(H_s + H_{\text{control}}\right)}{\Omega}, \tag{1}$$

where q (L^3T^{-1}) is the volumetric flux, A (L^2) is the area of the sink within the cell, K_s (LT^{-1}) is the saturated hydraulic conductivity of the soil, H_c (L) is the hydraulic head in the soil, H_s (L) is the hydraulic head in the drainpipe/ditch, H_{control} (L) is the control effect in controlled subsurface drainage (i.e., the elevation difference between the drain outlet and drainpipe in the cell when the outlet elevation is higher than the drainpipe elevation and 0 m otherwise), and Ω (L) is the entrance resistance. Note that flow to open ditches and subsurface drains is active only when H_c exceeds the sum of H_s and H_{control}, and water cannot flow from drains or ditches into the soil. Water can be removed through the open ditches as well as overland flow.

Water exchange rate between the pore systems is described as follows:

$$\tau = \gamma K_A |H_f - H_m|, \quad (2)$$

where τ (T^{-1}) is the water exchange rate between the systems (the direction of water flow is toward the lower hydraulic head), γ (L^{-2}) is the exchange coefficient, K_A (LT^{-1}) is the hydraulic conductivity of the pore system with higher hydraulic head, and H_f and H_m (L) are the hydraulic heads in the macropores and in the soil matrix, respectively.

3.2 | Model application

3.2.1 | Model setup and calibration

The model setup included the cultivated block and part of the adjacent forest area (Figure 1). Drainpipes were set into the block according to the actual drainage design. Ditch 1 had a depth of 1.5 m, Ditch 2 had a depth of 0.6 m, and the forest area was drained with five 0.7-m deep open ditches based on digital elevation model (National Land Survey of Finland, 2015). The pressure head in the drainpipes and ditches was assumed to be a constant of 0 m (the ditch water levels were not measured). This means that H_s in Equation (1) was treated as just the elevation head. The horizontal cell size of the 3D grid was 5 m × 5 m. The grid was arranged so that the elevation of the topmost grid cell of each column was set according to the topography. The cell thickness ranged from 0.02 m at the surface to 0.5 m at the bottom, and the total depth of the grid was a constant 3.4 m. The model had five soil layers: three peat layers and a mineral layer according to the soil samples, and a bottom layer. The block was divided into five areas with varying thickness of the lowest peat layer according to the GPR data. The forest area had a constant peat cover thickness, and the lowest peat layer was made thicker according to the average elevation difference between the forest and the block (1.2 m). To compensate for the increased peat thickness in the forest, the bottom layer thickness was reduced. Otherwise, the soil parameters and potential evapotranspiration parameters were the same for the block and the forest due to lack of measurements from the forest. The north-eastern and south-western boundaries (Figure 1) allowed groundwater outflow using a groundwater gradient equal to the soil surface gradient at the boundaries but no inflow (Turunen et al., 2013). Currently, the model output does not differentiate between groundwater outflows generated at different boundary segments. The south-eastern boundary and the north-western boundary below the ditch were impermeable. The bottom boundary was impermeable, and its elevation followed the soil surface elevation.

The WRC parameters (α and n in eq. 21 in van Genuchten [1980]) for the soil matrix were obtained by fitting the modeled WRC to the observed water retention values from the soil samples. van Genuchten parameters for the macropores were taken from previous studies of Turunen et al. (2013) and Salo et al. (2021).

Hourly timeseries of precipitation, air temperature, relative humidity, shortwave and longwave radiation components, wind speed, and potential evapotranspiration were used as the meteorological input for the model. Wind speed was measured at 16 m above the ground, so it was adjusted to the standard height of 2 m following the logarithmic wind speed profile above a short grassed surface suggested by Food and Agriculture Organization (FAO) guidelines (Allen et al., 1998). Potential evapotranspiration was determined with the Penman–Monteith equation (Allen et al., 1998), and the longwave radiation was based on the Stefan–Bolzmann law, following the FAO guidelines (Allen et al., 1998). Potential evapotranspiration was set to zero during snow cover, as the integrated snow model computes evaporation from the snowpack. Observed precipitation was adjusted by factors of 1.1 and 1.2 for simulated rainfall and snowfall, respectively (Førland et al., 1996). Following Turunen et al. (2015) and Salla et al. (2022), rooting depth was 0.05 m until the time of sowing, after which it grew linearly 0.01 m day^{-1} until harvest or until it reached the maximum value of 0.75 m where it remained until harvest. After harvest, it returned to 0.05 m. The rooting depth of 0.05 m was used to describe evaporation from the surface layer outside growing seasons.

The calibrated parameters consisted of saturated hydraulic conductivities, shares of macropores, exchange coefficients between the pore systems (Equation 2) (Table 1), and the drain resistance Ω (Equation 1). The share of macropores of the observed mineral layer was calibrated because the measured water content at 0.1 m pressure in that layer was higher than its measured total porosity. A condition of no macropores was set in the bottom layer based on the calibration and was numerically implemented in the model application by giving the pore systems identical properties, as setting the share of macropores explicitly to zero is not supported by the two-domain parameterization of the model. The calibration period was August 2018–February 2020, and the validation period was March 2020–October 2021. Only automatic observations were used in the calibration and validation. The parameters were manually calibrated, and the model performance was evaluated using Kling–Gupta efficiency (KGE) and mean absolute error (MAE) for hourly groundwater table depths at the OWs and hourly drain discharge. KGE combines

TABLE 1 Depths, saturated hydraulic conductivities (K_{sat}), residual water contents (θ_{res}), the van Genuchten parameters (α and n), shares of macropores, exchange coefficients, and total porosities of the soil layers.

Layer	Peat1	Peat2	Peat3	Mineral	Bottom
Depth (m)	0–0.25	0.25–0.35	0.35–0.60[a]	0.60[a]–1.10	1.10–3.40
$K_{sat,m}$ (m h^{-1})	0.00019	0.00023	0.00026	0.001	0.0001
$K_{sat,f}$ (m h^{-1})	1.7	1.6	0.9	0.006	–
$\theta_{res,m}$ (m^3 m^{-3})	0.04	0.05	0.10	0.14	0.10
α_m (1 m^{-1})	7.68	8.57	2.9	0.37	0.58
n_m (-)	1.16	1.13	1.14	1.79	1.12
$\theta_{res,f}$ (m^3 m^{-3})	0.1	0.1	0.1	0.1	0.01
α_f (1 m^{-1})	10	10	10	10	7
n_f (-)	1.8	1.8	1.8	1.8	2.0
Share of macropores (%)	9.2	8.6	4.6	0.1	0.0
Exchange coefficient γ (-)	0.9	0.9	0.9	0.1	–
Total porosity (%)	82.1	92.1	94.3	38.4	56.0
$K_{sat,total}$ (m h^{-1})	0.1566	0.1378	0.0461	0.0010	0.0001

Note: Subscripts m and f refer to soil matrix and macropores, respectively. The gray parameters were calibrated, yellow parameters were taken from literature (Salo et al., 2021; Turunen et al., 2013), and the green parameters were based on observations. The bottom row shows the total saturated hydraulic conductivities, that is, the weighted mean of conductivities in matrix and macropores with the pore system fractions as weights.

[a]In the model application, the depth of the interface between Peat3 and Mineral layers varied spatially between 0.55 m and 0.65 m.

evaluations of correlation, standard deviation, and mean (Knoben et al., 2019):

$$\mathrm{KGE} = 1 - \sqrt{(r-1)^2 + \left(\frac{\sigma_{sim}}{\sigma_{obs}} - 1\right)^2 + \left(\frac{\mu_{sim}}{\mu_{obs}} - 1\right)^2}, \quad (3)$$

where r is the linear correlation coefficient between observations and simulation, σ is the standard deviation, and μ is the mean. The subscripts sim and obs refer to simulation and observation, respectively. Correlation between a time series and observation is not defined if the time series has a constant value, but assuming the correlation as zero yields a natural benchmark for the constant time series of observation mean: $\mathrm{KGE} = 1 - \sqrt{2} \approx -0.4$ (Knoben et al., 2019). Another benchmark used by Knoben et al. (2019) is the midpoint between mean observation KGE (−0.4) and a perfect model KGE (1). In this study, KGE values are classified as weak (KGE ≤ 0.3) and satisfactory (KGE > 0.3).

3.2.2 | The effects of controlled drainage and inflow from the forest

The CD in the model followed the reported drainage system operation (Figure 3). The simulated effects of CD on groundwater table depths and drain discharge were quantified by subtracting the CD results from the conventional subsurface drainage (1.1-m drainage depth) results. The CD effect on groundwater table depths was averaged over the computational cells between the OWs. The CD effect on peat soil moisture was quantified by subtracting the results with conventional subsurface drainage from the results with CD. Regarding the CD effect on peat soil moisture, a weighted mean was taken at the locations of the groundwater observation tubes over the vertical column of peat cells and over both pore systems (matrix and macropores) at the OW 2 and OW 4. The peat cell thicknesses and pore system fractions were used as the weights.

The effect of inflow from the forest was quantified by comparing the initial simulation results to a scenario where the forest was excluded from the simulation and an impermeable boundary was placed on the north-eastern border of the block below Ditch 2. The effect on groundwater table depth was averaged over the study period and over computational cells having the same distance from the forest, gaining an average effect as a function of distance from the forest.

4 | RESULTS

4.1 | Model calibration and validation

The applied saturated hydraulic conductivities, van Genuchten water retention parameters, porosities, and exchange coefficients are listed in Table 1, where the calibrated parameters are marked with gray color. The calibration resulted in the peat layers having 3–4 orders of magnitude higher saturated hydraulic conductivities in macropores compared to the soil matrix, whereas the difference was smaller in the mineral layer. Macropores were excluded from the clayey bottom layer, as macropores with significantly higher conductivity compared to the matrix led to too efficient

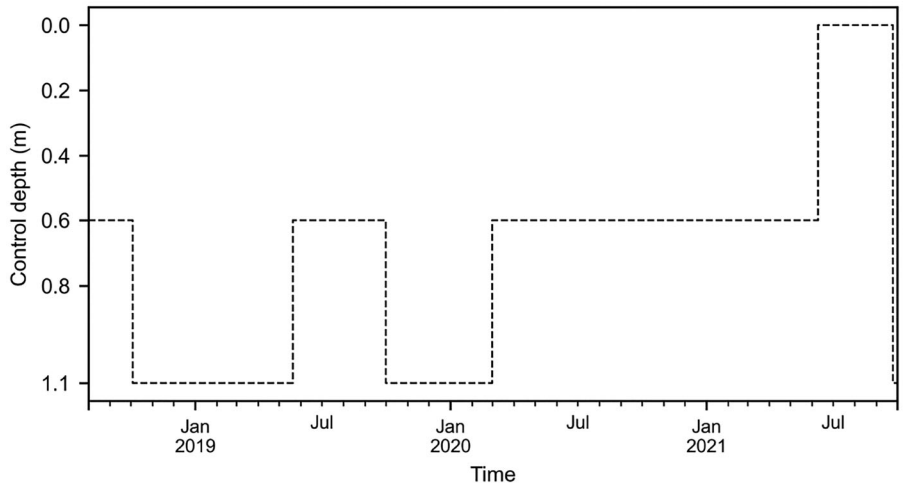

FIGURE 3 Control depth, that is, the depth of drain outlet from the soil surface in the controlled drainage well. The depth of 1.1 m means that no drainage control was used, and the depth of 0.0 m refers to an attempt to prevent all drain discharge.

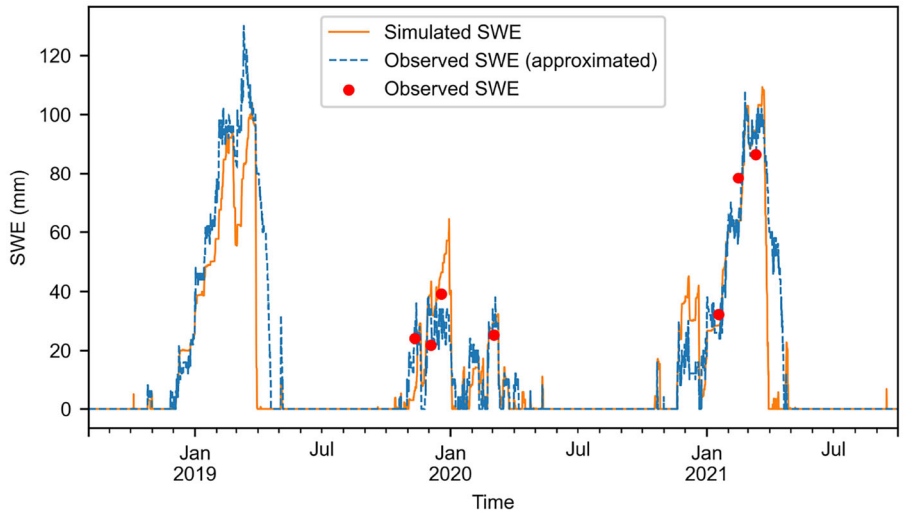

FIGURE 4 The simulated snow water equivalent (SWE), the SWE approximated from observed snow depth, and seven measured SWE values.

removal of water from the grid and too deep groundwater tables. Due to the high conductivities in the peat macropores, the total conductivities were on average 200 times larger in peat compared to the mineral and bottom layer. The drain resistance (Ω in Equation 1) was calibrated to a value of 0.6 m.

SWE computed by the model was compared to SWE approximated from snowpack thickness observations (Figure 4). The actual SWE measurements showed that the method to approximate SWE from snow depth gave credible values despite its crudeness. The SWE dynamics matched reasonably well during snow accumulation, but the simulation exhibited too fast melting in February and March of 2019 and March of 2021.

The observed and simulated groundwater table depths are shown as ranges in Figure 5, and the performance metrics are listed in Table 2. During the calibration period, the KGEs and MAEs were on average 0.52 and 0.17 m, respectively, indicating a satisfactory model performance. Still, during two timespans in the calibration period, October 2018–February 2019 and September 2019–October 2019, there were large differences between simulation and observations. Also, the differences in simulated and observed snowmelt events in 2019 were visible as mismatch in the groundwater table dynamics. During the validation period, the model performance decreased. The KGEs and MAEs were on average 0.16 and 0.19 m, respectively, and KGE remained above 0.3 only in the matrix in the OW 2. The KGE values decreased more in the OW 4 and the MAE values were 0.05–0.06 m higher than in OW 2. The observed groundwater tables were deeper in the OW 4 for most of the validation period, especially from September 2020 to May 2021 (seen as the relatively large observed range in Figure 5).

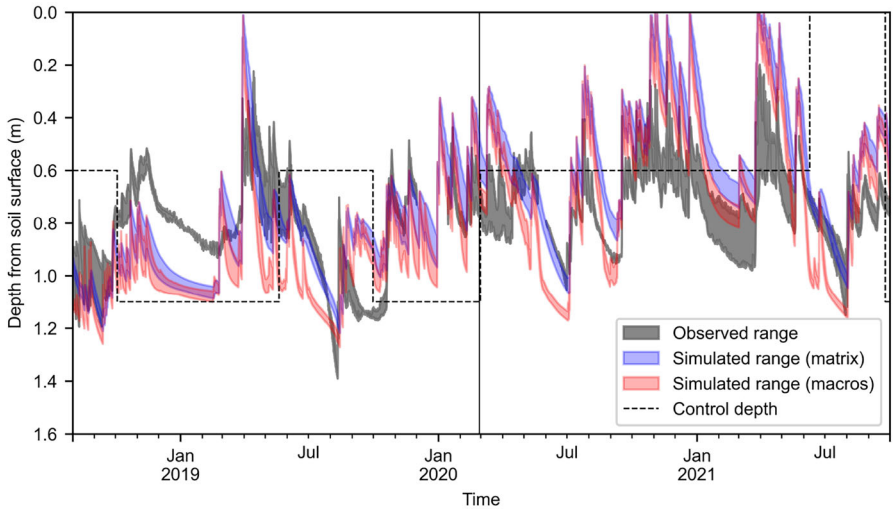

FIGURE 5 Observed range of groundwater table depths over the two observation wells and simulated range over all the grid cells between the observation wells (matrix and macropores), including the control depth. The vertical line separates the calibration period August 2018–February 2020 and the validation period March 2020–October 2021.

TABLE 2 Kling–Gupta efficiencies (KGE) and mean absolute errors (MAE) for groundwater table depths and drain discharge.

Variable	Efficiency value	Calibration	Validation
Groundwater table depths (observation well 2)	Matrix KGE	0.42	0.34
	Macropore KGE	0.45	0.21
	Matrix MAE	0.15 m	0.18 m
	Macropore MAE	0.18 m	0.15 m
Groundwater table depths (observation well 4)	Matrix KGE	0.65	0.13
	Macropore KGE	0.56	−0.04
	Matrix MAE	0.15 m	0.24 m
	Macropore MAE	0.18 m	0.20 m
Drain discharge	KGE	0.62	0.60
	MAE	0.03 mm h^{-1}	0.03 mm h^{-1}

The adjusted precipitation was 902 and 1108 mm during the calibration period and validation period, respectively, and the simulated actual evapotranspiration was on average 74% of the potential evapotranspiration (Figure 6a). The observed and simulated drain discharges are shown in Figure 6b,c, and the corresponding performance metrics are listed in Table 2. Cumulative curves are shown for hydrological years resetting in the beginning of September except in the beginning of the first and in the end of the third hydrological year, both of which have one extra month. Unlike with groundwater tables, the drain discharge performance was similar between the calibration and validation periods, the KGEs being 0.62 and 0.60, respectively. In the beginning of the calibration period, the model produced more drain discharge than what was observed (Figure 6b,c), even though the modeled water table was clearly lower than the measured water table (Figure 5). The simulated snowmelt event in February 2019 was visible as an early discharge event, and the total amount of snowmelt induced drain discharge was lower in the simulation. During the validation period, there were two observed drain discharge events that were not reproduced by the model: April–May 2020 and January–February 2021. Especially the measured discharge in February 2021 coincided with low observed water tables in comparison to simulation and control depth in Figure 5, suggesting a clear inconsistency between discharge and water table observations. The simulated snowmelt-induced drain discharge in the spring 2021 was again lower than observed, but the difference was smaller compared to the spring 2019. In June–September 2021, some drain discharge was observed despite high drainage outlet elevation during that time.

The simulated drain discharge was compared also to the scenario without the forest area (Figure 6b,c). Excluding the forest led to a much lower amount of drain discharge, the difference being on average 149 mm per hydrological year. The simulated amount of drain discharge without the forest was only 60% of what was observed. The simulated groundwater tables at the OWs were almost identical with and without the forest, as the average difference was less than 0.001 m. Figure 7 shows that the inflow from the forest reduced groundwater table depths in the proximity of the forest compared to the scenario with no forest, but with distances above 25 m from the forest, the impact on groundwater table depths was close to zero.

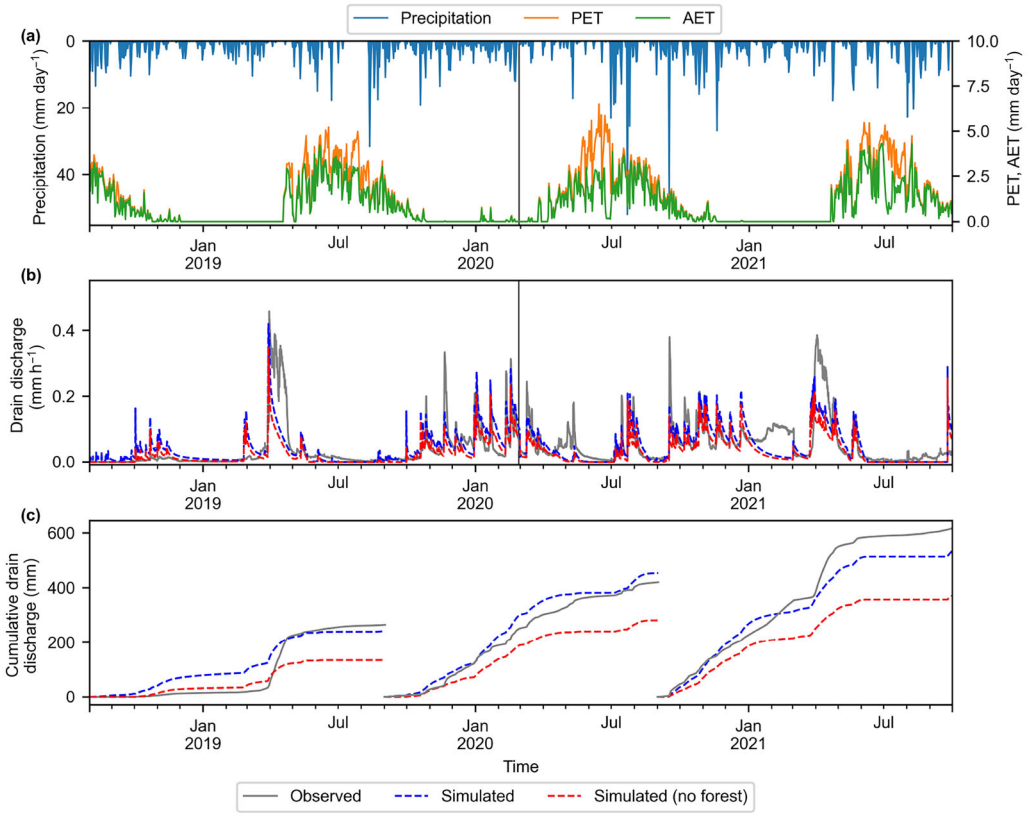

FIGURE 6 (a) Daily precipitation, potential evapotranspiration (PET), and simulated actual evapotranspiration (AET); (b) hourly observed and simulated (with and without the forest area) drain discharge; and (c) the corresponding cumulative values. In (a), evaporation from snowpack is not included, as it is computed separately by the integrated snow model. In (c), the cumulative curves reset in the beginning of September, expect in the beginning of the first and in the end of the third hydrological year, both of which have one extra month.

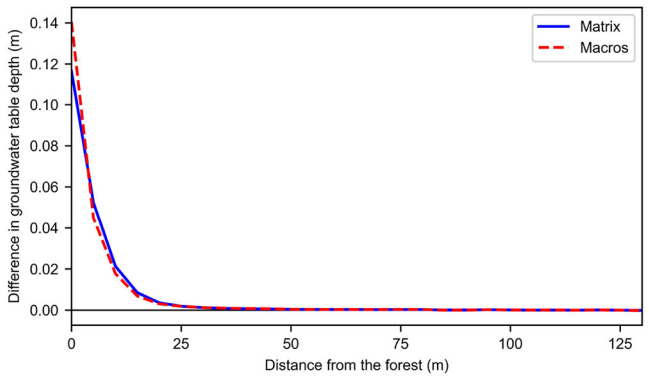

FIGURE 7 The average difference between groundwater table depths in the block without the forest and with the forest included in the model as a function of distance from the forest. Positive values indicate shallower groundwater tables with the forest included.

At the depth of 0.1 m, the simulated soil moisture in peat at the locations of the OWs varied between 29% and 82% (total porosity at that depth) in the matrix and between 11% and 82% in the macropore domain. The average values were 65% and 28% in the matrix and macropores, respectively. 86% of the measured soil moisture values at 0.1 m were between the simulated matrix moisture and macropore moisture, and the rest were below that range. At the depth of 0.5 m, the simulated soil moisture in peat varied between 82% and 94% (total porosity at that depth) in the matrix and between 19% and 94% in the macropore domain. The average values were 91% and 53% in the matrix and macropores, respectively. 69% of the measured soil moisture values at 0.5 m were between the simulated matrix moisture and macropore moisture, and the rest were below that range.

4.2 | The effects of controlled drainage

After the modeling setup was tested against field observations, we simulated the potential of CD to influence groundwater levels, peat moisture, and drain discharge in field scale by comparing the CD scheme to conventional subsurface drainage (Figure 8). During summer months (June–August), when the control depth was set from 1.1 to 0.6 m, groundwater table depths were reduced on average by 0.1 and 0.08 m in the soil matrix and macropores, respectively. These CD effects were lowest in 2018 (0.05 and 0.03 m) and highest in 2020 (0.12 and 0.11 m), which correlates negatively

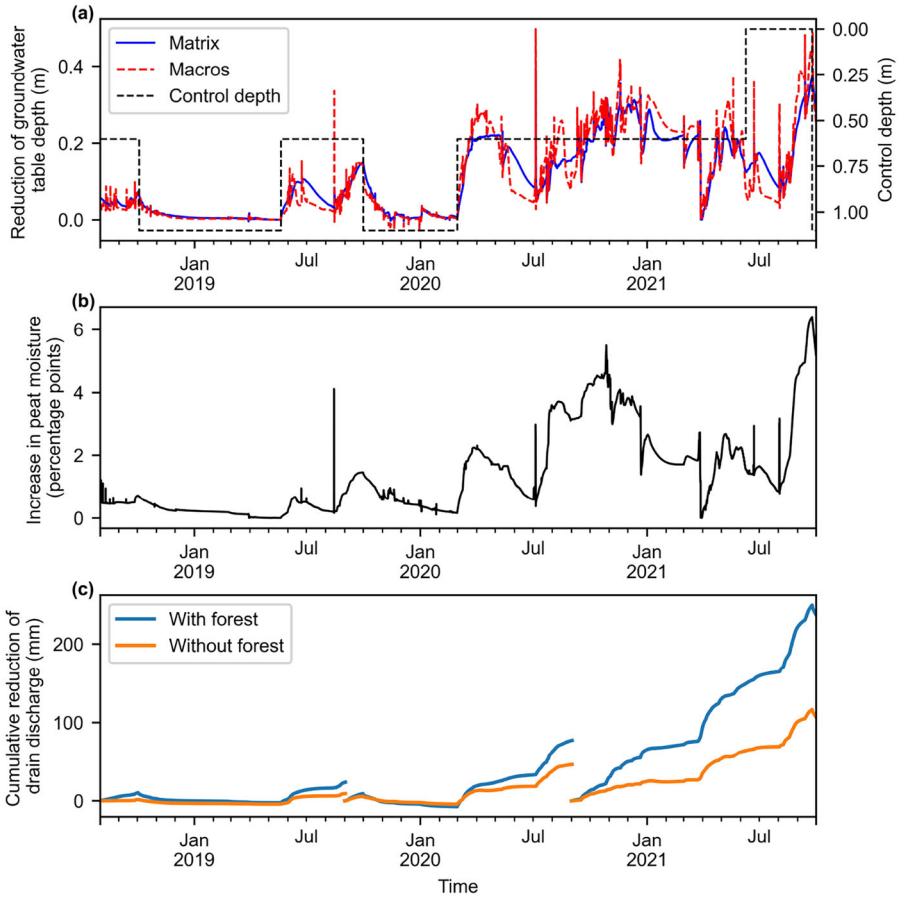

FIGURE 8 The simulated (a) reduction of groundwater table depths in the soil matrix and macropores (averaged over the grid cells between the observation wells), (b) change in peat moisture (averaged over the observation well locations and depth range of 0–0.65 m), and (c) cumulative reduction of drain discharge caused by controlled drainage in comparison to conventional drainage.

with average groundwater table depths (Figure 5). During other months with control depth of 0.6 m, the average CD effects on groundwater tables were 0.18 and 0.19 m in the soil matrix and macropores, respectively. Control depth of 0 m (i.e., blocking all drain discharge) led to the highest average effect during summer months (0.17 and 0.16 m in the soil matrix and macropores, respectively). The changes in peat moisture reflected the CD effect on groundwater tables. The changes were small, as the control depth of 0.6 m resulted only in an average change of 1.8 percentage points, which was due to peat maintaining high moisture content even without CD, especially in the deeper layers.

During the first half of the study period, when CD was applied only during growing seasons, the CD effects on drain discharge were small, and taking the control off led to higher drain discharge compared to conventional drainage (seen as negative slopes in Figure 8c). During the second half of the study period, CD was applied for a longer period while the groundwater tables and precipitation were also higher, which resulted in much larger reduction of drain discharge. Excluding the forest area from the simulation did not have an impact on how CD affected groundwater levels or peat moisture at the OWs, but the absolute reductions of drain discharge were twice as large with the forest (Figure 8c). The relative reductions of drain discharge were 22% and 17% with the forest included and excluded, respectively.

The spatial distributions of the CD effects on matrix and macropore groundwater table depths are shown in Figure 9, averaged over the times when the control depth was set to 0.6 m. The blue color depicts how much the average groundwater table depths were reduced by CD at different locations, darker shades indicating larger effect. The CD effects on groundwater table depths in the field block correlated negatively with the soil surface elevation, that is, larger effects taking place at lower surface elevations. Higher effects can also be seen in the drainpipe locations as inclined stripes. The average effects over the field block were 0.16 m and 0.18 m in the matrix and macropores, respectively, and the effect was visible circa 30 m into the forest area. The highest effects took place at the border between the block and the forest.

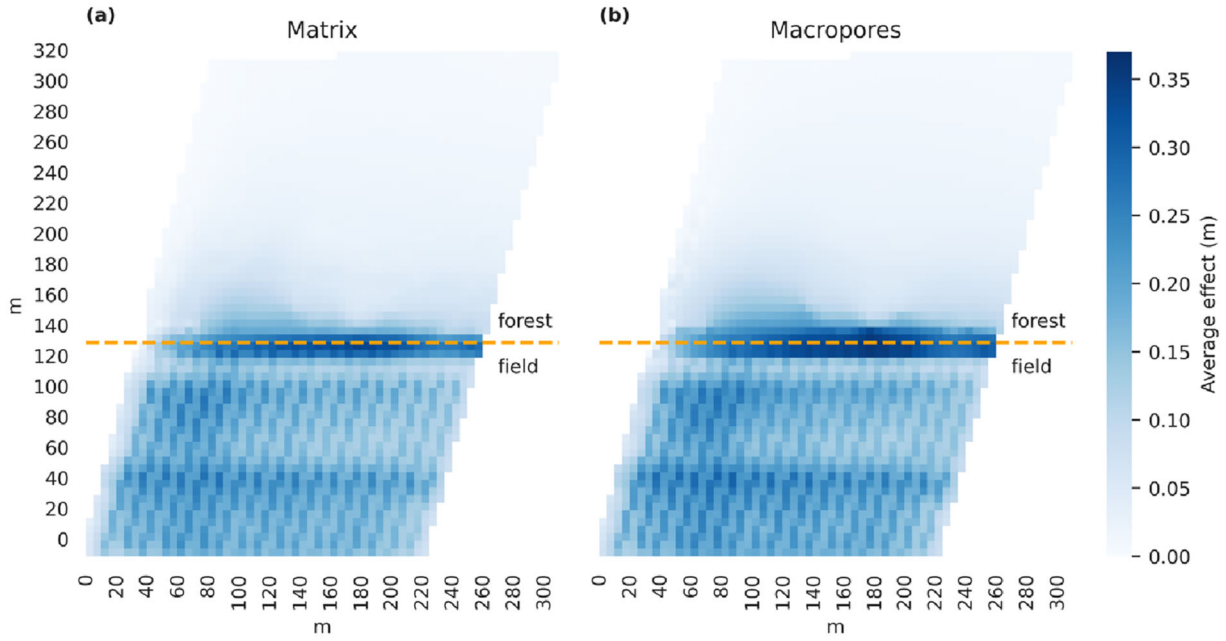

FIGURE 9 The average effect of the controlled drainage scheme on groundwater table depths (a) in the soil matrix and (b) macropores compared to conventional drainage during the times when the control depth was set to 0.6 m. Larger values mean larger average reductions of groundwater table depth.

5 | DISCUSSION

5.1 | Model parameterization, performance, and uncertainties

FLUSH provided a transparent tool to quantify the hydrology of the drained peatland in combination with a limited hydrological dataset. The main implication from the model calibration and validation process was that replication of quick drain discharge was not possible without inclusion of macropore domain in the model parameterization of the peatland field. The role of macropores in simulated drain discharge dynamics has been highlighted also by Akai et al. (2008). The second observation was that the measured volume of drain discharge could not be simulated without inclusion of subsurface flow entering the field from the adjacent forest. The novelty of our computational exercise is to demonstrate these processes that are not clearly visible in the dataset alone.

Peatlands are heterogenous in terms of hydraulic properties (Rezanezhad et al., 2016; Wang et al., 2021). However, due to spatially lacking data on soil properties, the soil parameters used in this study did not vary horizontally, apart from the differences in soil layer thickness and topography. In Wang et al. (2021), spatial autocorrelations of saturated hydraulic conductivity and macroporosity were classified as weak in natural end extremely degraded peat sites and strong and moderate, respectively, in a moderately degraded site. The autocorrelations of the van Genuchten parameters were mostly moderate. Due to Wang et al. (2021) having only three sites, it cannot be concluded how this autocorrelation is related to the degree of peat degradation. While having soil measurements only from one location is a source of uncertainty in this study, it is not unreasonable to assume that the spatial autocorrelations of the applied parameters were not high, and thus, there was no strong systematic variation within the field which would cause a large difference in the model results.

Peatlands are often described as anisotropic in terms of hydraulic properties (Rezanezhad et al., 2016; Wang et al., 2020). However, this is not always the case. In Kiuru et al. (2022), there was only slight anisotropy in the top peat layer, while no anisotropy was found in deeper more degraded layers. In this study, vertical and horizontal saturated hydraulic conductivities were not measured separately, and the same values were applied in the model for both directions. While saturated hydraulic conductivities in the matrix were based on measurements, the ones in macropores were calibrated, and thus, their values were affected by possible anisotropy of the site. Models are never perfect representations of reality, and we suspect that the cost of increasing the amount of calibrated saturated hydraulic conductivities of peat would be larger than the benefit, especially in a field with a shallow peat cover. As a result of the calibration process, the peat layers obtained high saturated hydraulic conductivities in macropores in relation to the measured conductivities in the peat matrix. This reflects the common characteristics of peat, which is reported

to have strong dual porous nature (Rezanezhad et al., 2016). The importance of macropores in hydrological modeling of peat has been noted also by Dettmann et al. (2014). Due to the thick peat cover in the upslope forest area and the highly conductive macropores of peat, there appeared to be a large inflow across the forest–field interface, which is in line with the findings of Lambert et al. (2022). Unique hydraulic properties of macropores are difficult to determine with measurements, but their inclusion and parameterization in the model is crucial due to their dominant role in soil water flow. The saturated hydraulic conductivities of peat macropores were calibrated in this study, but their water retention parameters were taken from a mineral soil study (Salo et al., 2021). The bottom layer was calibrated to have no macropores, as conductive macropores allowed too efficient removal of water from the grid. This connects to uncertainties related to the boundary conditions and water levels in the open ditches.

The model performance in terms of groundwater level simulation was more satisfactory during the calibration than the validation period. The validation performance decreased due to lower simulated depths compared to the observations, particularly in the OW 4. A possible reason for the different observed behavior of the wells is transient and spatially varying hydrological interaction between the block and its environment caused by, for example, changes in local preferential flow dynamics due to freeze-thaw cycles or anthropogenic impacts (e.g., Hare et al., 2017). Another possible reason is the scale mismatch between the point measurement and the grid-scale model result, as the observed values depend on the location of the well in relation to the spatial differences in the macropore networks (Bouma et al., 1980). Drain discharge is aggregated over the drainage system, which makes it less sensitive to field-scale spatial heterogeneity, and with respect to drain discharge, the model performance for the calibration and validation periods was equally satisfactory.

Hydrological measurement campaigns spanning for years are challenging in Nordic peatlands. Soil freezing and thawing may lead to spatially variable changes in the groundwater level, observation tubes may be blocked due to presence of ice in the tube, and snowmelt can cause floods disturbing discharge measurements. There were seeming inconsistencies in the hydrological datasets used in this study, that is, groundwater table and drain discharge observations, which became obvious when set against the model results. During conventional drainage in October–November 2018, the observed groundwater levels were at depth of 0.5–0.7 m, but very little drain discharge was measured. This contrasts with times when larger quantity of drain discharge was measured even though the observed groundwater levels were approximately at the same level and the control depth was elevated to 0.6 m from the soil surface (e.g., May 2020). In January–February 2021, there was a large amount of drain discharge measured while the observed groundwater levels were more than 0.15 m below the control depth. In our model, drain discharge is generated always when the water table is above the drainpipe depth. These inconsistencies suggest issues in the hydrological measurement systems or in the CD management, but they can be partly caused by complex hydrological behavior between the block and the forest. There were nine manual groundwater table depth observations during the study period (four in the OW 2 and five in the OW 4), all of them fitting reasonably well to the automatic observations. However, in April 2018, before the study period, there were four manual observations made in the OW 2, which were 35–40 cm lower than the automatic observations, raising some concern about the reliability of the automatic groundwater table observations. The automatic drain discharge observations had an error ranging between 10% and 30% in 2017 compared to manual measurements, but this error was unsystematic and did not likely lead to large bias on an annual basis. During the study period, the original drain discharge measurement data exhibited some unrealistic spikes (50–100 mm h^{-1}), which were assumed to be measurement artifacts caused by flooding at the observation system. These spikes were pruned off, but it is still uncertain whether and to what extent flooding or other disturbances affected the rest of the discharge dataset.

Seibert et al. (2018) argued that the model performance should be evaluated based on what can be expected or what is possible for a certain dataset. The hydrological simulations and observations in this study exhibited inconsistencies, although it is difficult to say exactly how much the model performance was limited by the accuracy of observations. The model bound the measurements together and retained computational consistency between the hydrometeorological variables, thus providing a reference to assess the quality and consistency of the independent observations. Keeping the limitations of the observation dataset in mind, the model setup was considered adequate in describing the field hydrology and to be used in studying the effects of CD in the field. Drained peatlands are significant CO_2 hotspots and hydrology is a major driver of the biochemical processes, but mechanistic descriptions of peatland hydrology are still rare. This study aimed to improve our understanding of this important but under-researched topic. The strength of the applied approach was to combine the different measurements into a single computational framework, which has been benchmarked in previous field-scale studies (e.g., Turunen et al., 2013, 2015; Warsta et al., 2013). The approach produces systemic and transparent computational information regarding the hydrology of the peatland field, which would be difficult to produce only empirically.

5.2 | The hydrological effects of controlled drainage in the peat field

Water management is proposed to be among the most effective ways to mitigate peat decomposition and high greenhouse gas emissions from cultivated peatlands (Evans et al., 2021; Wen et al., 2020), but hydrological impacts of CD have been rarely quantified. During summer months (June–August), setting the control depth from 1.1 to 0.6 m resulted in average reductions of 0.1 and 0.08 m in the soil matrix and macropore groundwater tables, respectively. Already this magnitude is relevant regarding reductions in peat degradation (Evans et al., 2021). Higher effects were gained outside the summer months. It is clear that often the CD target could not be met, as groundwater tables were much of the time deeper than the control depth. The CD effects depend on the hydrological conditions (Joel et al., 2009; Salo et al., 2021), and the lower CD effect during summer was caused by relatively deep groundwater tables and high evapotranspiration losses. With deeper groundwater tables, CD had less potential to affect their depth, and with groundwater tables below the drainage level, CD had no impact at all. Another factor is the duration of the control period, as longer periods of CD can allow more water to accumulate into the soil, leading to higher groundwater levels (Salla et al., 2022).

The effects of CD on groundwater tables showed spatial variability in the field block. As expected, slightly higher CD effects took place at the drainpipe locations. The CD effects also correlated negatively with the soil surface elevation. This can be explained by drainpipes having a constant depth from the soil surface in the model. At locations with lower soil surface elevation, there was a larger difference between the drainpipe elevation and the outlet elevation, leading to higher potential CD impact. The largest effects in the block took place next to the forest area, which is in line with the simulated groundwater tables being higher close to the forest.

It should be noted that changes in the soil moisture profile caused by changes in groundwater levels are significantly weaker when the distance from the groundwater table increases (Orellana et al., 2012). Thus, the CD effect on peat moisture and degradation might be low in areas with shallow peat cover and deep groundwater tables. Our simulation showed the CD effect on peat moisture to be mostly less than 5 percentage points, but one reason for this was the high water retention capacity of the peat matrix. The soil matrix of the deeper parts of the peat cover often remained nearly saturated outside the summer months even with conventional drainage. Lower peat moisture took place during the summer months, at times when the groundwater tables were deep, and the CD effect on groundwater tables was limited, leading to low effects on peat moisture as well.

The results showed that the CD effect on drain discharge depends on the hydrometeorological conditions, particularly the position of groundwater table relative to the control depth, and the duration of control measures. Drain discharge is directly linked with leaching of nutrients from the field into surface waters (Carstensen et al., 2019; Yli-Halla, Lötjönen, Kekkonen et al., 2022). When CD was applied only during growing seasons, the effect on drain discharge was small, and drain discharge was temporarily larger compared to conventional drainage when control was taken off. Still, retaining water in the field during growing seasons can increase the efficiency of nutrient uptake of the plants, leading to lower nutrient load on surface water (Wesström & Messing, 2007).

5.3 | The effects of hydrological connections

Hydrological connections have been found to affect the water balance of drained peatlands (Koivusalo et al., 2008). Also, Mahmood et al. (2023) and Turunen et al. (2015) showed how topography and adjacent hillslopes can be important drivers in drain discharge generation. While it has been reported that CD can increase lateral flow from field areas (Youssef et al., 2021), hydrological impacts of lateral inflow in controlled drained peatlands have not been previously analyzed. Our simulation results showed how hydrological connections between the field and the adjacent forest area can induce high drain discharge at the field. In this study, both absolute and relative reductions of drain discharge caused by CD were larger with the forest included in the simulations.

The inflow from the forest had a relevant impact on groundwater tables within about 25 m from the forest, but farther away at the OWs it had no impact on groundwater tables or how they were affected by CD. This implies inflow into a field might not be important regarding peat degradation in field-scale, but it depends on how fast the incoming water is removed from the field via drainage system, evapotranspiration, or lateral groundwater outflow.

6 | CONCLUSIONS

A 3D modeling system and its application added value to limited hydrological observations and revealed how hydrological processes in a cultivated peatland responded to CD. The simulation showed that CD raised groundwater tables to an extent that has been shown in literature to be relevant in reducing peat degradation and CO_2 emissions. However, a high groundwater table in the field was not maintained with CD during the summertime with high evapotranspiration losses. The effect of CD on peat moisture was small, mainly due to the high water retention capacity of peat.

The adjacent forest area had a strong impact on the field water balance. The impact of the inflow on groundwater table

depths was spatially limited to the proximity of the forest, whereas the inflow strongly increased the amount of drain discharge. The impact of CD on groundwater table and soil moisture was insensitive to forest inflow, whereas the control impact on drain discharge was greatly dependent on the presence of forest inflow. Hydrological connections affecting the field water balance complicate interpretations made from hydrometeorological data alone and highlight the need to view the field as a part of its environment with varying topography and land use.

AUTHOR CONTRIBUTIONS

Aleksi Salla: Methodology; visualization; writing—original draft. **Heidi Salo**: Methodology; writing—review and editing. **Mika Tähtikarhu**: Methodology; writing—review and editing. **Hannu Marttila**: Writing—review and editing. **Miika Läpikivi**: Visualization; writing—review and editing. **Maarit Liimatainen**: Writing—review and editing. **Timo Lötjönen**: Writing—review and editing. **Harri Koivusalo**: Methodology; supervision; writing—review and editing.

ACKNOWLEDGMENTS

This study was funded by Maa- ja vesitekniikan tuki ry and adheres to Digital Waters (DIWA, 359248). Flagship funded by the Research Council of Finland. Luke acknowledges Council of Oulu region (361/2021); Kone foundation, Finland (grant No. 201802192); Suoviljelysyhdistys, Finland; Centre for Economic Development, Transport and the Environment, Finland (POPELY/2790/2020); European Regional Development Fund (grant No. A78444); Rural development program, Finland (grant No. 83215, 190444); Drainage Foundation sr; and MMM, the Ministry of Agriculture and Forestry of Finland. Computation resources for running the simulations were provided by CSC–IT Center for Science Ltd. Thanks to Markus Saari from the University of Oulu for producing the GPR data.

CONFLICT OF INTEREST STATEMENT

The authors declare no conflicts of interest.

ORCID

Aleksi Salla https://orcid.org/0000-0002-3344-8050
Miika Läpikivi https://orcid.org/0000-0001-9877-0289

REFERENCES

Akai, O., Fox, G. A., & Šimůnek, J. (2008). Numerical simulation of flow dynamics during macropore—Subsurface drain interactions using HYDRUS. *Vadose Zone Journal*, *7*, 909–918. https://doi.org/10.2136/vzj2007.0148

Allen, R., Pereira, L., Raes, D., & Smith, M. (1998). *Crop evapotranspiration—Guidelines for computing crop water requirements* (Irrigation and Drainage Paper No. 56). FAO.

Bouma, J., Dekker, L. W., & Haans, J. C. F. M. (1980). Measurement of depth to water table in a heavy clay soil. *Soil Science*, *130*, 264–270. https://doi.org/10.1097/00010694-198011000-00006

Carstensen, M. V., Børgesen, C. D., Ovesen, N. B., Poulsen, J. R., Hvid, S. K., & Kronvang, B. (2019). Controlled drainage as a targeted mitigation measure for nitrogen and phosphorus. *Journal of Environmental Quality*, *48*, 677–685. https://doi.org/10.2134/jeq2018.11.0393

Coelho, B. B., Bruin, A. J., Staton, S., & Hayman, D. (2020). Sediment and nutrient contributions from subsurface drains and point sources to an agricultural watershed. *Air, Soil and Water Research*, *3*. https://doi.org/10.1177/ASWR.S4471

Dettmann, U., Bechtold, M., Frahm, E., & Tiemeyer, B. (2014). On the applicability of unimodal and bimodal van Genuchten–Mualem based models to peat and other organic soils under evaporation conditions. *Journal of Hydrology*, *515*, 103–115. https://doi.org/10.1016/j.jhydrol.2014.04.047

Dou, X., Shi, H., Li, R., Miao, Q., Yan, J., Tian, F., & Wang, B. (2022). Simulation and evaluation of soil water and salt transport under controlled subsurface drainage using HYDRUS-2D model. *Agricultural Water Management*, *273*, 107899. https://doi.org/10.1016/j.agwat.2022.107899

Evans, C. D., Peacock, M., Baird, A. J., Artz, R. R. E., Burden, A., Callaghan, N., Chapman, P. J., Cooper, H. M., Coyle, M., Craig, E., Cumming, A., Dixon, S., Gauci, V., Grayson, R. P., Helfter, C., Heppell, C. M., Holden, J., Jones, D. L., Kaduk, J., … Morrison, R. (2021). Overriding water table control on managed peatland greenhouse gas emissions. *Nature*, *593*, 548–522. https://doi.org/10.1038/s41586-021-03523-1

Førland, E. J., Allerup, P., Dahlström, B., Elomaa, E., Jónsson, T., Madsen, H., Perälä, J., Rissanen, P., Vedin, H., & Vejen, F. (1996). *Manual for operational correction of Nordic precipitation data* (Report No. 24/96). Norwegian Meteorological Institute.

Gerke, H. H., & van Genuchten, M. Th. (1993). A dual-porosity model for simulating the preferential movement of water and solutes in structured porous media. *Water Resources Research*, *29*, 305–319. https://doi.org/10.1029/92WR02339

Haahti, K., Warsta, L., Kokkonen, T., Younis, B. A., & Koivusalo, H. (2016). Distributed hydrological modeling with channel network flow of a forestry drained peatland site. *Water Resources Research*, *52*, 246–263. https://doi.org/10.1002/2015WR018038

Hare, D. K., Boutt, D. F., Clement, W. P., Hatch, C. E., Davenport, G., & Hackman, A. (2017). Hydrogeological controls on spatial patterns of groundwater discharge in peatlands. *Hydrology and Earth System Sciences*, *21*, 6031–6048. https://doi.org/10.5194/hess-21-6031-2017

Hill, D. F., Burakowski, E. A., Crumley, R. L., Keon, J., Hu, J. M., Arendt, A. A., Wikstrom Jones, K., & Wolken, G. J. (2019). Converting snow depth to snow water equivalent using climatological variables. *The Cryosphere*, *13*, 1767–1784. https://doi.org/10.5194/tc-13-1767-2019

Holden, J. (2009). Flow through macropores of different size classes in blanket peat. *Journal of Hydrology*, *364*, 342–348. https://doi.org/10.1016/j.jhydrol.2008.11.010

Holden, J., Chapman, P. J., & Labadz, J. C. (2004). Artificial drainage of peatlands: Hydrological and hydrochemical process and wetland restoration. *Progress in Physical Geography: Earth and Environment*, *28*, 95–123. https://doi.org/10.1191/0309133304pp403ra

Ikkala, L., Ronkanen, A. K., Utriainen, O., Kløve, B., & Marttila, H. (2021). Peatland subsidence enhances cultivated lowland flood risk. *Soil & Tillage Research*, *212*, 105078. https://doi.org/10.1016/j.still.2021.105078

Isomäki, K., Salla, A., Salo, H., & Koivusalo, H. (2024). Hydrological effects of open ditch damming and controlled subsurface drainage in a Nordic agricultural field. *Hydrology Research*, *55*, 112–127. https://doi.org/10.2166/nh.2024.053

Jarvis, N. J. (2007). A review of non-equilibrium water flow and solute transport in soil macropores: Principles, controlling factors and consequences for water quality. *European Journal of Soil Science*, *58*, 523–546. https://doi.org/10.1111/j.1365-2389.2007.00915.x

Joel, A., Wesström, I., & Messing, I. (2009). Mapping suitability of controlled drainage using spatial information of topography, land use and soil type, and validation using detailed mapping, questionnaire and field survey. *Hydrology Research*, *40*, 406–419. https://doi.org/10.2166/nh.2009.054

Kęsicka, B., Kozłowski, M., & Stasik, R. (2023). Effectiveness of controlled tile drainage in reducing outflow and nitrogen at the scale of the drainage system. *Water*, *15*, 1814. https://doi.org/10.3390/w15101814

Kiuru, P., Palviainen, M., Grönholm, T., Raivonen, M., Kohl, L., Gauci, V., Urzainki, I., & Laurén, A. (2022). Peat macropore networks—New insights into episodic and hotspot methane emission. *Biogeosciences*, *19*, 1959–1977. https://doi.org/10.5194/bg-19-1959-2022

Knisel, W. G., & Turtola, E. (2000). Gleams model application on a heavy clay soil in Finland. *Agricultural Water Management*, *43*, 285–309. https://doi.org/10.1016/S0378-3774(99)00067-0

Knoben, W. J. M., Freer, J. E., & Woods, R. A. (2019). Technical note: Inherent benchmark or not? Comparing Nash-Sutcliffe and Kling-Gupta efficiency scores. *Hydrology and Earth System Sciences*, *23*, 4323–4331. https://doi.org/10.5194/hess-23-4323-2019

Koivusalo, H., Ahti, E., Lauren, A., Kokkonen, T., Karvonen, T., Nevalainen, R., & Finer, L. (2008). Impacts of ditch cleaning on hydrological processes in a drained peatland forest. *Hydrology and Earth System Sciences*, *12*, 1211–1227. https://doi.org/10.5194/hess-12-1211-2008

Koivusalo, H., Heikinheimo, M., & Karvonen, T. (2001). Test of a simple two-layer parameterisation to simulate energy balance and temperature of a snowpack. *Theoretical and Applied Climatology*, *70*, 65–79. https://doi.org/10.1007/s007040170006

Laiho, R. (2006). Decomposition in peatlands: Reconciling seemingly contrasting results on the impacts of lowered water levels. *Soil Biology & Biochemistry*, *38*, 2011–2024. https://doi.org/10.1016/j.soilbio.2006.02.017

Lambert, C., Larocque, M., Gagné, S., & Garneau, M. (2022). Aquifer-peatland hydrological connectivity and controlling factors in boreal peatlands. *Frontiers in Earth Science*, *10*, Article 835817. https://doi.org/10.3389/feart.2022.835817

Larsson, M. H., & Jarvis, N. J. (1999). Evaluation of a dual-porosity model to predict field-scale solute transport in a macroporous soil. *Journal of Hydrology*, *215*, 153–171. https://doi.org/10.1016/S0022-1694(98)00267-4

Li, J., Wang, X., Bai, L., & Mao, X. (2017). Quantification of lateral seepage from farmland during maize growing season in arid region. *Agricultural Water Management*, *191*, 85–97. https://doi.org/10.1016/j.agwat.2017.06.006

Limpens, J., Berendse, F., Blodau, C., Canadell, J. G., Freeman, C., Holden, J., Roulet, N., Rydin, H., & Schaepman-Strub, G. (2008). Peatlands and the carbon cycle: From local processes to global implications—A synthesis. *Biogeosciences*, *5*, 1475–1491. https://doi.org/10.5194/bg-5-1475-2008

Mahmood, H., Schneider, R. J. M., Frederiksen, R. R., Christiansen, A. V., & Stisen, S. (2023). Using jointly calibrated fine-scale drain models across Denmark to assess the influence of physical variables on spatial drain flow patterns. *Journal of Hydrology: Regional Studies*, *46*, 101353. https://doi.org/10.1016/j.ejrh.2023.101353

Maljanen, M., Sigurdsson, B. D., Guðmundsson, J., Óskarsson, H., Huttunen, J. T., & Martikainen, P. J. (2010). Greenhouse gas balances of managed peatlands in the Nordic countries—Present knowledge and gaps. *Biogeosciences*, *7*, 2711–2738. https://doi.org/10.5194/bg-7-2711-2010

Muma, M., Rousseau, A. N., & Gumiere, S. J. (2017). Modeling of subsurface agricultural drainage using two hydrological models with different conceptual approaches as well as dimensions and spatial scales. *Canadian Water Resources Journal [Revue canadienne des ressources hydriques]*, *42*, 38–53. https://doi.org/10.1080/07011784.2016.1231014

National Land Survey of Finland. (2015). *Elevation model 2 m*. https://www.maanmittauslaitos.fi/en/maps-and-spatial-data/datasets-and-interfaces/product-descriptions/elevation-model-2-m

Oleszczuk, R., Lång, K., Szajdak, L., Höper, H., & Maryganova, V. (2008). Impacts of agricultural utilization of peat soils on the greenhouse gas balance. In M. Strack (Ed.), *Peatlands and climate change* (pp. 70–97). International Peat Society.

Orellana, F., Verma, P., Loheide, II, S. P., & Daly, E. (2012). Monitoring and modeling water-vegetation interactions in groundwater-dependent ecosystems. *Reviews of Geophysics*, *50*, https://doi.org/10.1029/2011RG000383

Päivänen, J. (1973). Hydraulic conductivity and water retention in peat soils. *Acta Forestalia Fennica*, *129*, Article 7563. https://doi.org/10.14214/aff.7563

Pham, T., Yli-Halla, M., Marttila, H., Lötjönen, T., Liimatainen, M., Kekkonen, J., Läpikivi, M., Klöve, B., & Joki-Tokola, E. (2023). Leaching of nitrogen, phosphorus and other solutes from a controlled drainage cultivated peatland in Ruukki, Finland. *Science of the Total Environment*, *904*, 166769. https://doi.org/10.1016/j.scitotenv.2023.166769

Querner, E. P., Mioduszewski, W., Povilaitis, A., & Slesicka, A. (2010). Modelling peatland hydrology: Three cases from Northern Europe. *Polish Journal of Environmental Studies*, *19*, 149–159.

Querner, E. P., Jansen, P. C., van den Akker, J. J. H., & Kwakernaak, C. (2012). Analysing water level strategies to reduce soil subsidence in Dutch peat meadows. *Journal of Hydrology*, *446–447*, 59–69. https://doi.org/10.1016/j.jhydrol.2012.04.029

Regina, K., Budiman, A., Greve, M. H., Grønlund, A., Kasimir, Å., Lehtonen, H., Petersen, S. O., Smith, P., & Wösten, H. (2016). GHG mitigation of agricultural peatlands requires coherent policies. *Climate Policy*, *16*, 522–541. https://doi.org/10.1080/14693062.2015.1022854

Rezanezhad, F., Price, J. S., Quinton, W. L., Lennartz, B., Milojevic, T., & Van Cappellen, P. (2016). Structure of peat soils and implications for water storage, flow and solute transport: A review update for geochemists. *Chemical Geology*, *429*, 75–84. https://doi.org/10.1016/j.chemgeo.2016.03.010

Salla, A., Salo, H., & Koivusalo, H. (2022). Controlled drainage under two climate change scenarios in a flat high-latitude field. *Hydrology Research*, *53*, 14–28. https://doi.org/10.2166/nh.2021.058

Salo, H., Mellin, I., Sikkilä, M., Nurminen, J., Äijö, H., Paasonen-Kivekäs, M., Virtanen, S., & Koivusalo, H. (2019). Performance of subsurface drainage implemented with trencher and trenchless machineries. *Agricultural Water Management*, *213*, 957–967. https://doi.org/10.1016/j.agwat.2018.12.010

Salo, H., Salla, A., & Koivusalo, H. (2021). Seasonal effects of controlled drainage on field water balance and groundwater levels. *Hydrology Research*, *52*, 1633–1647. https://doi.org/10.2166/nh.2021.056

Salo, H., Warsta, L., Turunen, M., Paasonen-Kivekäs, M., Nurminen, J., & Koivusalo, H. (2015). Development and application of a solute transport model to describe field-scale nitrogen processes during autumn rains. *Acta Agriculturae Scandinavica, Section B—Soil & Plant Science*, *65*, 30–43. https://doi.org/10.1080/09064710.2014.971861

Seibert, J., Vis, M. J. P., Lewis, E., & van Meerveld, H. J. (2018). Upper and lower benchmarks in hydrological modelling. *Hydrological Processes*, *32*, 1120–1125. https://doi.org/10.1002/hyp.11476

Skaggs, T. H., Trout, T. J., Šimůnek, J., & Shouse, P. J. (2004). Comparison of HYDRUS-2D simulations of drip irrigation with experimental observations. *Journal of Irrigation and Drainage Engineering*, *130*, 304–310. https://doi.org/10.1061/(ASCE)0733-9437(2004)130:4(304)

Turunen, M., Warsta, L., Paasonen-Kivekäs, M., & Koivusalo, H. (2017). Computational assessment of sediment balance and suspended sediment transport pathways in subsurface drained clayey soils. *Soil & Tillage Research*, *174*, 58–69. https://doi.org/10.1016/j.still.2017.06.002

Turunen, M., Warsta, L., Paasonen-Kivekäs, M., Nurminen, J., Alakukku, L., Myllys, M., & Koivusalo, H. (2015). Effects of terrain slope on long-term and seasonal water balances in clayey, subsurface drained agricultural fields in high latitude conditions. *Agricultural Water Management*, *150*, 139–151. https://doi.org/10.1016/j.agwat.2014.12.008

Turunen, M., Warsta, L., Paasonen-Kivekäs, M., Nurminen, J., Myllys, M., Alakukku, L., Äijö, H., Puustinen, M., & Koivusalo, H. (2013). Modeling water balance and effects of different subsurface drainage methods on water outflow components in a clayey agricultural field in boreal conditions. *Agricultural Water Management*, *121*, 135–148. https://doi.org/10.1016/j.agwat.2013.01.012

van Genuchten, M. Th. (1980). A closed-form equation for predicting the hydraulic conductivity of unsaturated soils. *Soil Science Society of America Journal*, *44*, 892–898. https://doi.org/10.2136/sssaj1980.03615995004400050002x

Wang, M., Liu, H., & Lennartz, B. (2021). Small-scale spatial variability of hydro-physical properties of natural and degraded peat soils. *Geoderma*, *399*, 115–123. https://doi.org/10.1016/j.geoderma.2021.115123

Wang, M., Liu, H., Zak, D., & Lennartz, B. (2020). Effect of anisotropy on solute transport in degraded fen peat soils. *Hydrological Processes*, *34*, 2128–2138. https://doi.org/10.1002/hyp.13717

Warsta, L. (2011). *Modelling water flow and soil erosion in clayey, subsurface drained agricultural fields* [Doctoral dissertation, Aalto University].

Warsta, L., Karvonen, T., Koivusalo, H., Paasonen-Kivekäs, M., & Taskinen, A. (2013). Simulation of water balance in a clayey, subsurface drained agricultural field with three-dimensional FLUSH model. *Journal of Hydrology*, *476*, 395–409. https://doi.org/10.1016/j.jhydrol.2012.10.053

Wen, Y., Zang, H., Ma, Q., Freeman, B., Chadwick, D. R., Evans, C. D., & Jones, D. L. (2020). Impact of water table levels and winter cover crops on greenhouse gas emissions from cultivated peat soils. *Science of the Total Environment*, *719*, 135130. https://doi.org/10.1016/j.scitotenv.2019.135130

Wesström, I., & Messing, I. (2007). Effects of controlled drainage on N and P losses and N dynamics in a loamy sand with spring crops. *Agricultural Water Management*, *87*, 229–240. https://doi.org/10.1016/j.agwat.2006.07.005

Yli-Halla, M., Lötjönen, T., Kekkonen, J., Virtanen, S., Marttila, H., Liimatainen, M., Saari, M., Mikkola, J., Suomela, R., & Joki-Tokola, E. (2022). Thickness of peat influences the leaching of substances and greenhouse gas emissions from a cultivated organic soil. *Science of the Total Environment*, *806*, 150499. https://doi.org/10.1016/j.scitotenv.2021.150499

Yli-Halla, M., Lötjönen, T., Liimatainen, M., & Joki-Tokola, E. (2022). *Ohutturpeiselta pellolta tuleva ympäristökuormitus: Ruukin koekentän perustaminen ja ensimmäisiä tuloksia veteen ja ilmakehään päätyvästä kuormituksesta*. Luonnonvara-ja biotalouden tutkimus 50. Natural Resources Institute Finland. http://urn.fi/URN:ISBN:978-952-380-450-0

Youssef, M. A., Liu, Y., Chescheir, G. M., Skaggs, R. W., & Negm, L. M. (2021). DRAINMOD modeling framework for simulating controlled drainage effect on lateral seepage from artificially drained fields. *Agricultural Water Management*, *254*, 106944. https://doi.org/10.1016/j.agwat.2021.106944

Zhou, X., Helmers, M., & Qi, Z. (2013). Modeling of subsurface tile drainage using MIKE SHE. *Applied Engineering in Agriculture*, *29*, 865–873. https://doi.org/10.13031/aea.29.9568

How to cite this article: Salla, A., Salo, H., Tähtikarhu, M., Marttila, H., Läpikivi, M., Liimatainen, M., Lötjönen, T., & Koivusalo, H. (2024). Simulating controlled drainage and hydrological connections in a cultivated peatland field. *Vadose Zone Journal*, e20387. https://doi.org/10.1002/vzj2.20387